SOIL FERTILITY AND CROP NUTRITION

Application of Machine Learning Methodologies for Predicting Corn Economic Optimal Nitrogen Rate

Zhisheng Qin,* D. Brenton Myers, Curtis J. Ransom, Newell R. Kitchen, Sang-Zi Liang, James J. Camberato, Paul R. Carter, Richard B. Ferguson, Fabian G. Fernandez, David W. Franzen, Carrie A.M. Laboski, Brad D. Malone, Emerson D. Nafziger, John E. Sawyer, and John F. Shanahan

ABSTRACT

Determination of in-season N requirement for corn (*Zea mays* L.) is challenging due to interactions of genotype, environment, and management. Machine learning (ML), with its predictive power to tackle complex systems, may solve this barrier in the development of locally based N recommendations. The objective of this study was to explore application of ML methodologies to predict economic optimum nitrogen rate (EONR) for corn using data from 47 experiments across the US Corn Belt. Two features, a water table adjusted available water capacity (AWC_{wt}) and a ratio of in-season rainfall to AWC_{wt} ($RAWC_{wt}$), were created to capture the impact of soil hydrology on N dynamics. Four ML models—linear regression (LR), ridge regression (RR), least absolute shrinkage and selection operator (LASSO) regression, and gradient boost regression trees (GBRT)—were assessed and validated using "leave-one-location-out" (LOLO) and "leave-one-year-out" (LOYO) approaches. Generally, RR outperformed other models in predicting both at planting and split EONR times. Among the 47 tested sites, for 33 sites the predicted split EONR using RR fell within the 95% confidence interval, suggesting the chance of using the RR model to make an acceptable prediction of split EONR is ~70%. When RR was used to test split EONR prediction with input weather features surrogated with 10 yr of historical weather data, the model demonstrated robustness (MAE, 33.6 kg ha^{-1}; $R^2 = 0.46$). Incorporating mechanistically derived hydrological features significantly enhanced the ability of the ML procedures to model EONR. Improvement in estimating in-season soil hydrological status seems essential for success in modeling N demand.

Core Ideas

- A Machine Learning approach was innovatively used to predict corn EONR.
- Two features were created to approximate hydrological conditions for modeling EONR.
- Soil hydrology conditions were found essential in successful modeling in-season EONR.

THE DEVELOPMENT of locally based precision N recommendation algorithms is complicated by soil, weather, management, and genetic interactions (Tremblay et al., 2012). A recent paper (Morris et al., 2018) provides a history of this process. Many N recommendation models have been developed to help producers maximize corn yield by predicting the economic optimum nitrogen rate (EONR). The earliest N recommendation tools were developed based on "yield goal" assumption. The yield goal–based N recommendations were the predominant approach from the 1970s until the early 2000s, when the Maximum Return to N (MRTN) system of N recommendations was developed for a large area of the US Corn Belt (Sawyer et al., 2006). This system uses regionally specific N response functions within state boundaries, determined by researchers across corn-growing states and growing seasons, to calculate a net profit return to N curve. The suggested N rate is identified where the net return to N reaches a maximum.

Remote sensing–based approaches have also been used for N management. Several different approaches and indices to determine spectral signatures of corn canopies have been proposed (Rhezali et al., 2018). Based on the reflectance signatures, various algorithms and protocols were developed to determine EONR for corn (Barker and Sawyer, 2010; Dellinger et al., 2008; Holland and Schepers, 2013; Kitchen et al., 2010; Lukina et al., 2001; Raun et al., 2001, 2002; Scharf and Lory, 2009; Schmidt et al., 2009; Tubaña et al., 2008).

Z. Qin, D.B. Myers, S. Liang, P.R. Carter, B.D. Malone, Dupont Pioneer, 8325 NW 62nd Ave., Johnston, IA 50131; C.J. Ransom, Univ. of Missouri, 269 Agric. Eng. Bldg., Columbia, MO 65211; N.R. Kitchen, USDA–ARS Cropping Systems and Water Quality Research Unit, 243 Agric. Eng. Bldg., Columbia, MO 65211; J.J. Camberato, Purdue Univ., Lilly 3-365, West Lafayette, IN 47907; R.B. Ferguson, Univ. of Nebraska, Keim 367, Lincoln, NE 68583; F.G. Fernandez, Univ. of Minnesota, 1991 Upper Buford Circle, St. Paul, MN 55108; D.W. Franzen, North Dakota State Univ., P.O. Box 6050, Fargo, ND 58108; C.A.M. Laboski, Univ. of Wisconsin-Madison, 1525 Observatory Dr., Madison, WI 53706; E.D. Nafziger, Univ. of Illinois, W-301 Turner Hall, 1102 S. Goodwin, Urbana, IL 61801; J.E. Sawyer, Iowa State Univ., 3208 Agronomy Hall, Ames, IA 50011; J.F. Shanahan, Fortigen, 6807 Ridge Rd, Lincoln, NE 68512. Received 29 Mar. 2018. Accepted 30 July 2018. *Corresponding author (jason.qing@pioneer.com).

Application of computer simulation models is a recent development to provide site-specific in-season N recommendations (Basso et al., 2012; Dumont et al., 2016; Puntel et al., 2016). Such models integrate soil, weather, crop, and management into a large interconnected set of mathematical equations that calculate important physical and physiological processes involved in crop development and yield formation (Morris et al., 2018). Nitrogen demand predicted by computer simulation models is based on explicit model-generated estimates of N supply, N loss, and crop N uptake at the time of in-season application. Adapt-N (Melkonian et al., 2008) and Maize-N (Setiyono et al., 2011) are two N recommendation systems based on computer simulation models.

Other N recommendation approaches include soil N testing (Dahnke and Vasey, 1973; Magdoff et al., 1984; Schepers et al., 1986) and plant tissue testing (Ma et al., 2005; Scharf, 2001). These recommendation approaches rely on simple tests and often limited information available up to the time fertilization is performed (e.g., pre-plant, sidedress), yet they are often judged against EONR, which encompasses full-season effects of G × E × M factors, where G represents genetic characteristics and phenotype expressions, such as degree days required for flowering and maturity; E represents environmental variables, including weather, soil, and topographic information that is relevant to the crop–soil N cycle; and M represents management variables, such as planting date, N application dates, etc. Recommendations that better embrace the complexity of G × E × M factors are needed.

An alternative modeling approach for determining the corn N fertilizer recommendations that we explore here entails the use of machine learning (ML) methodologies. Machine learning belongs to the artificial intelligence domain of the computer science field. Machine learning algorithms use modern computing power to directly "learn" from data without being explicitly programmed by any predetermined models (Samuel, 1959). In general, there are two categories of ML: supervised learning and unsupervised learning. Supervised learning involves learning mapping functions from input variables to output (or target) variables. Supervised learning algorithms are most commonly used by ML practitioners to solve real-world problems. Some common supervised learning algorithms include regression, random forests for regression and classification, and support vector machines for classification. Unsupervised learning involves inferring a function that describes the structure of data that are unlabeled (i.e., there are no labeled outputs). The most common unsupervised learning algorithm is clustering analysis.

The distinction between statistics and ML is sometimes blurry, but there are certain characteristics that differentiate ML from statistics. Usually there are more input variables (features) involved in ML than traditional statistics. These features may or may not physically explain the target variable and significance of the individual feature is less important. Machine learning is more concerned with boosting the predictive power of the model using combinations of features. Especially when many features are used to build an ML model, overfitting or an overspecialization to the data used to generate the model may be an issue. Machine learning approaches often guard against this problem by using techniques like regularization and cross-validation. Although it is not the case with this study, ML learning may involve a larger amount of data than traditional statistics can handle.

Machine learning algorithms of many types exist, but most iteratively optimize algorithmic structures and parameters to predict the target variable from the input features. One advantage of applying ML to model a complex system is that ML bypasses all intermediate processes otherwise explicitly explained by a mechanistic modeling system, such as Maize-N, and makes a prediction directly based on input information. In this study, a few ML algorithms were used to learn the behavior of an underlying N process from input feature data (i.e., soil, weather, and management information) collected in conjunction with the target variable (in this case measured EONR).

Numerous studies have applied ML to answer agronomic questions (Gonzalez-Sanchez et al., 2014; Jeong et al., 2016; Karimi et al., 2008; McQueen et al., 1995; Morellos et al., 2016; Rumpf et al., 2010; Shekoofa et al., 2014). There has been no documented attempt to apply ML to predict season-long corn N demand. A likely reason is that ML has larger data requirements than typically measured in traditional agronomic experiments. In addition, G × E × M interactions drive soil N supply and plant N uptake, so the modeling approach needs to be trained with a large set of potential environmental conditions to accurately predict N needs. Typically, controlled N experiments developed to predict in-season N demand do not cover a sufficiently large number of different environments. An exception is the research of Tremblay et al. (2012), which examined the results of 51 N trials conducted across a wide geographic region. Their meta-analysis (not ML techniques) revealed relationships between corn yield response to N with soil texture and rainfall patterns. Xie et al. (2013) also conducted a meta-analysis based on data collected from multiyear N trials at 60 locations in Quebec; finding corn yield response to in-season N application was reduced with low accumulated corn heat units, low precipitation, and uneven precipitation before sidedressing. Soil variables were not examined in this study.

In 2014, a public-private collaborative project entitled "Performance and Refinement of N Fertilization Tools" was launched by DuPont Pioneer, USDA–ARS Cropping Systems and Water Quality Unit, and eight participating public land-grant midwestern universities, including University of Illinois, Iowa State University, University of Minnesota, University of Missouri, University of Nebraska, North Dakota State University, Purdue University, and University of Wisconsin-Madison (Kitchen et al., 2017). One objective of this study was to evaluate corn response to N fertilizer timing and rate, soil properties, and weather conditions with standardized protocols and methods across a wide range of corn-growing environments in the midwestern United States. The project lasted 3 yr (2014–2016) and generated multiple datasets that provide valuable information for testing ML methods for predicting in-season corn N needs.

The objective of this study was to develop ML models to predict EONR at planting and for split application timings and to test the in-season application of the model using historical weather and model-derived features.

MATERIALS AND METHODS
Experimental Design and Site Level Economic Optimum N Rate Description

Details on the field research across the eight states in the project are presented in Kitchen et al. (2017). In general, two sites

were selected each year from each state based on contrasting soil productivity. Individual principal investigators decided if new sites were to remain on the same farm or if different farms were to be chosen, but in all cases they were unique fields. In total, 49 corn N response trials were selected. Locations encompassed a major portion of the Corn Belt, representing a wide range of soils and climatic conditions across six North America level II ecoregions (temperate prairies, west central semiarid prairies, south central semiarid prairies, central US plains, southeastern US plains, and mixed wood plains) (Commission for Environmental Cooperation, 1997). Across all locations, a consistent randomized complete block design with N timing and rate treatments replicated four times was used (Table 1). Treatments 1 through 8 tested N response to a planting time N application; Treatments 1, 2, and 9 through 14 evaluated N response for a split application with 45 kg N ha^{-1} at planting and the remainder as a sidedress N application around the V9 corn development stage. Treatment 1 (0 N treatment) was included with both N application timings. Hybrids differed among locations based on the typical maturity rating of hybrids used for the region. Average research area size per site was 0.4 ha to minimize soil and landscape variability within the experiments. Grain mass from each plot was measured after plant physiological maturity by hand- or combine harvesting. Grain yields were then adjusted to a standard moisture of 155 g kg^{-1}.

A quadratic-plateau model using SAS NLIN proc (SAS Institute, Cary, NC) was used to describe yield response to N rate for data of each treatment block within each field. To derive site-level EONR, yield and N data from all blocks for each site were used to fit the quadratic-plateau model (Kitchen et al., 2017) for each N application timing. To reduce data noise due to within-field variability, site level EONR was used in this study.

Among the 49 corn N response trials, 47 sites were used for further analysis. We removed two locations from the analysis (SCAL 2015 and Amenia 2016; see Table 1 of Kitchen et al. [2017] for site details) because of concerns about data reliability. For SCAL 2015, measured N response was compromised by the carryover effect of hail-damaged soybean plants of the previous season. For Amenia 2016, a urea and ammonium fertilizer was errantly applied in June, resulting in invalid yield response data for EONR calculation.

Environmental Data, Feature Extraction, and Selection

Weather data from each research site were obtained using onsite automatic U30 HOBO weather stations (Onsite Corp., Bourne, MA). Raw temperature and rainfall observations taken by the sensor every 15 min were summarized to maximum temperature, minimum temperature, and total precipitation on a daily basis. The summarized daily data were then quality checked against interpolated temperature data and multiradar multisensor rainfall data (The National Severe Storms Lab, NOAA). Any outliers and missing values were identified and replaced by the interpolated temperature or multiradar multisensor rainfall. The Bristow–Campbell equation (Bristow and Campbell, 1984) was used to calculate daily global solar radiation based on daily maximum temperature, minimum temperature, and rainfall. The Bristow–Campbell model was parameterized based on ground observational data collected

Table 1. Nitrogen treatments to test yield response to at-planting N application (1–8) and split applied with sidedress at V9 ± 1 leaf stage (1, 2, 9–14) across 49 Corn Belt locations.

Treatment	N at planting	Sidedress N	Total N
	kg N ha^{-1}		
1	0	0	0
2	45	0	45
3	90	0	90
4	135	0	135
5	180	0	180
6	225	0	225
7	270	0	270
8	315	0	315
9	45	45	90
10	45	90	135
11	45	135	180
12	45	180	225
13	45	225	270
14	45	270	315

from 239 weather stations across contiguous US states during 1961 to 1990 (Renewable Resources Data Center, Golden, CO).

Soil profile samples were taken from each of the four blocks of the project sites in the spring before planting and N application. Sampling depths were partitioned by natural soil horizons. Soil data used in this analysis included texture (sand, clay, and silt percent), percent organic matter, cation exchange capacity, and bulk density. These samples were further processed and analyzed to generate soil hydraulic and nutrient information (Kitchen et al., 2017). Annual minimum water table depth was extracted from the Soil Survey Geographic Database SSURGO (Natural Resources Service, USDA) for each site.

A common first step in the development of an ML model is to engineer or extract n-dimensional input features (Xs) to capture useful information that contributes to the predicted value (y). Based on the measured data, the geospatial location of the experiments, and experimental metadata (e.g., planting date and comparative relative maturity), we developed or transformed base data into a range of input features that correlate to physical, chemical, and physiological processes in the corn cropping system (Table 2).

Weather features were created for each site-year combination by aggregating weather data into five periods that characterize corn development based on planting date, intermediate phenological stages, and measured maturity (Table 3). The first period (P1) encompasses January first through planting. Weather conditions in this period determine planting time N and soil water status. Periods 2 through 5 represent the complete corn life cycle, which was divided into early and late vegetative stages (Periods 2 and 3) and early and late reproductive stages (Periods 4 and 5). Daily maximum and minimum temperatures were averaged to obtain daily average temperatures. Daily average temperatures and daily total solar radiation during each of the five periods were averaged to create temperature and radiation features. Daily precipitation data were summed to obtain total precipitation for each of the five periods. Fifteen weather features tied to crop phenology were created in total.

To use the EONR values for an in-season recommendation, in-season weather features are needed up to the time of yield realization. However, future weather events are unknown at the

Table 2. Weather, soil, and management data used to extract candidate input features.

Weather data	Soil data	Management data†
Daily maximum temperature, °C	Sand, silt, and clay, %	Planting date, DOY
Daily minimum temperature, °C	Organic matter	N application date, DOY
Daily total precipitation, mm	Bulk density	Hybrid maturity group, CRM
Daily total global solar radiation, MJ M^{-2}	Cation exchange capacity	Physiological maturity date, DOY
	Water table depth, mm	

† CRM, comparative relative maturity; DOY, day of year.

Table 3. Definition of periods for aggregating weather data to create weather features.

Period	Definition	Approximate crop stage
1	1 Jan. to planting	–
2	First quarter of crop cycle	Planting to V7
3	Second quarter of crop cycle	V7–R1
4	Third quarter of crop cycle	R1–R3
5	Fourth quarter of crop cycle	R3–R6

time of N application. To represent the inherent stochasticity of weather outcomes for the unknown portion of the growing season, we developed weather feature data for the period after N application date of the study year using the last 10 yr of historical weather data for each site. This resulted in a separate set of weather features for each historical year. Physiological maturity dates needed to identify the phenologically significant periods were simulated based on tested hybrids and planting dates for each historical season using DSSAT Ceres Maize 4.0 model. Genetic coefficients used were previously parameterized for Pioneer hybrids (Wei et al., 2009).

Soil features were created using depth-weighted averages of measured soil data up to 1 m, assuming corn root activities mainly occur within this depth across US Corn Belt. To account for diminishing root length with increased soil depth, three weights were used to aggregate soil property measurements throughout the profile: 0.5 for depths of 0 to 0.3 m, 0.3 for depths of 0.3 to 0.6 m, and 0.2 for depths 0.6 to 1 m. This approach allows the model to represent the effect of soil attributes in the primary root zone and reduces the need to include extra model features for multiple soil profile layers.

In addition to soil features created using measured soil data, two more features were created to represent field-level soil hydrological conditions in late spring and early summer: water table adjusted available water capacity (AWC$_{wt}$) and a ratio of cumulative in-season rainfall to AWC$_{wt}$ (RAWC$_{wt}$). We created these two features based on two considerations: (i) weather is typically wet during late spring and early summer across much of the US Corn Belt, and (ii) excessive moisture trapped in fine-textured soils (e.g., silty clay, clay loam, etc.) causes temporarily raised water tables and saturated soils, resulting in N loss due to denitrification or leaching. It is assumed under wet conditions that the amount of N lost is negatively correlated to the ability of a soil to hold water above the saturated zone, approximated by water table depth in this study.

Water table adjusted available water capacity was formulated as:

$$AWC_{wt} = AWC \times Depth_{wt} \quad [1]$$

where AWC is the available water capacity calculated from the measured soil texture and organic matter data by pedotransfer functions (Saxton and Rawls, 2006), and Depth$_{wt}$ is the

minimum water table depth in late spring and early summer obtained from SSURGO. One meter was set as the maximum water table depth to avoid overestimation of water holding capacity in the root zone.

The ratio of in-season rainfall to AWC$_{wt}$ (RAWC$_{wt}$) is another feature created to account for the effect of in-season rainfall on N loss considering soil water holding capacity. It was formulated as:

$$RAWC_{wt} = \frac{Rain_{\_inseason}}{AWC_{wt}} \quad [2]$$

where Rain$_{\_inseason}$ represents cumulative rainfall from planting time through maturity.

A large RAWC$_{wt}$ value indicates high in-season rainfall compounded with reduced AWC$_{wt}$, increasing the probability of N loss due to denitrification or leaching. For a wet season with high in-season rainfall, denitrification may happen in fine-textured soils with small AWC$_{wt}$, whereas leaching is more likely to occur in coarse-textured soils also having small AWC$_{wt}$. Due to the small plot size of the trial, topographic effects on AWC$_{wt}$ were not discussed in this study.

Management features included planting date, N application date (both planting time and sidedress application dates), and physiological maturity date. These dates were represented by number of days of the year in numeric values. In addition, an indicator variable was created to flag N application time, with 1 indicating planting-time application and 2 indicating sidedress-time application.

Some candidate features are more relevant than others when predicting EONR. Moreover, some features, such as sand percent and available water content, are highly correlated, which could cause overfitting of the model. To mitigate this and to improve prediction efficiency and accuracy, a recursive feature elimination procedure (Guyon et al., 2002) was used to recursively remove features that are less important and likely redundant. The recursive feature elimination algorithm is first trained on an initial set of normalized features to obtain standard model coefficients (e.g., the coefficients of a linear model) or feature importance; then the feature with the least importance is eliminated from current feature set. This feature elimination process is recursively performed to obtain a smaller feature set that includes a combination of features that mostly contribute to the prediction of the target variable. In this study, the desired number of features was determined by recursively evaluating the model's predicted R^2 value to ensure elimination of a feature would not compromise the model's predictability. In all, 22 features were selected to build a model for in-season N prescription (Table 4).

In some cases, the relationships between the selected input features and observed EONR were nonlinear. For this reason, second-degree polynomial terms were created to reflect nonlinearity of the relationships. The second-degree polynomial terms

Table 4. Input features selected by using recursive feature elimination for economic optimum N rate models.

Feature name	Description
N_time	N application timing (i) at planting or (ii) split application around V9
N_app_DOY	N application date, represented by day of year
Temp_1	Average air temperature during first period (1 Jan. to planting)
Temp_2	Average air temperature during second period (planting to V7)
Temp_3	Average air temperature during third period (V7–R1)
Temp_4	Average air temperature during fourth period (R1–R3)
Temp_5	Average air temperature during fifth period (R3–R6)
Precp_1	Total precipitation during first period (1 Jan. to planting)
Precp_2	Total precipitation during second period (planting to V7)
Precp_3	Total precipitation during third period (V7– R1)
Precp_4	Total precipitation during fourth period (R1–R3)
Precp_5	Total precipitation during fifth period (R3–R6)
SolarRad_1	Average solar radiation during first period (1 Jan. to planting)
SolarRad_2	Average solar radiation during second period (planting to V7)
SolarRad_3	Average solar radiation during third period (V7– R1)
SolarRad_4	Average solar radiation during fourth period (R1–R3)
SolarRad_5	Average solar radiation during fifth period (R3–R6)
CEC	Cation exchange capacity
OM	Organic matter
BD	Bulk density
AWC$_{wt}$	Available water capacity adjusted by water table depth
RAWC$_{wt}$	Ratio of in-season rainfall to AWC$_{wt}$

of those selected input variables were included in the input feature matrix for evaluation.

Machine Learning Algorithms and Model Evaluation

Four ML algorithms were tested for modeling EONR. These algorithms include linear regression (LR), ridge regression (RR), least absolute shrinkage and selection operator (LASSO), and gradient boost regression trees (GBRTs).

Linear Regression

Linear regression assumes the input variables have a Gaussian distribution. It is also assumed that input variables are relevant to the output variable and are not highly correlated with each other. The form of LR model is:

$$Y = \theta_0 + \theta_1 x_1 + \theta_2 x_2 + \ldots + \theta_n x_n \qquad [3]$$

where Y is the target variable, $x_1 \ldots x_n$ are input variables, and $\theta_1 \ldots \theta_n$ are coefficients.

To solve for the coefficients, the following cost function is minimized:

$$J = \sum_{i=1}^{n} \left(y_i - \sum_{j=1}^{p} x_{ij}\theta_j \right)^2 \qquad [4]$$

where J is the cost function, y_i is the vector of target variables, x_{ij} is the input variable matrix, and θ_j is the vector of coefficients.

With LR, no regularization factor is included to correct model overfitting, which is a concern for this dataset because some input features may not meet the assumptions that the input variables are uncorrelated. Also, the ratio of the number of training examples to the number of parameters is relatively low, especially

when second-degree polynomial terms of input features are incorporated, causing the parameter matrix to double in size.

Ridge Regression

Ridge regression is a technique used to create parsimonious models when a large number of features are present. It functions by adding a regularization component to avoid model overfitting. Ridge regression performs L2 regularization, which penalizes the coefficients by adding the square of the magnitude of the coefficient to the cost function:

$$J = \sum_{i=1}^{n} \left(y_i - \sum_{j=1}^{p} x_{ij}\theta_j \right)^2 + \lambda \sum_{j=1}^{p} \theta_j^2 \qquad [5]$$

where $\lambda \sum_{j=1}^{p} \theta_j^2$ is the regularization component, and λ is a regularization factor, which can be optimized by examining validation error.

LASSO Regression

The least absolute shrinkage and selection operator (LASSO) is a modification of LR. Similar to RR, LASSO penalizes the magnitude of coefficients to avoid overfitting. The LASSO regression performs L1 regularization (i.e., it adds a factor designated the sum of the absolute value of the coefficients into the optimization objective):

$$J = \sum_{i=1}^{n} \left(y_i - \sum_{j=1}^{p} x_{ij}\theta_j \right)^2 + \lambda \sum_{j=1}^{p} \left| \theta_j \right| \qquad [6]$$

where $\lambda \sum_{j=1}^{p} \left| \theta_j \right|$ is the regularization component, which is a summation of the absolute values of the feature coefficients.

Gradient Boosted Regression Trees

Gradient boosted regression trees (GBRT) is an ML regression model where decision trees, which individually are weak predictors due to their tendency to overfit the data (Rokach and Maimon, 2008), are combined to form a more robust model in an iterative fashion (boosting). For this study, we used XGBoost (eXtreme Gradient Boosting), a popular implementation of GBRT available through the open-source python package XGBoost (Chen and Guestrin, 2016). The model offers many opportunities for regularization, including regularization on the number of leaves and individual leaf weights, shrinkage of newly added trees, and column subsampling. The hyperparameters of these regularization options were determined through cross-validation.

For Ridge and LASSO regression models, an array of regularization factors (λ) were tested to select the optimal value to achieve the highest R^2 and lowest mean absolute error (MAE) and RMSE from cross-validation. Model hyperparameters for XGBoost were tuned using Bayesian optimization (Snoek et al., 2012).

Model Performance Evaluation

Three statistics were used to evaluate the performance of the four types of models: R^2, MAE, and RMS.

The R^2 evaluates the proportion of variance in the target variable explained by the model.

$$R^2 = 1 - \frac{\sum_i \left(y_i - \hat{y}_i \right)^2}{\sum_i \left(y_i - \overline{y} \right)^2} \qquad [7]$$

Where y_i is the observed target variable value, $\hat{y}_i$ is the predicted target variable value, and $\overline{y}$ is the mean of observed target variable value.

Mean absolute error measures the average magnitude of the errors between predicted and observed target variable values. It is the average of the absolute differences between prediction and actual observations. Because all individual errors have equal weight in the calculation, MAE is less sensitive to large prediction errors.

$$\text{MAE} = \frac{1}{n} \sum_{i=1}^{n} \left| y_i - \hat{y}_i \right| \qquad [8]$$

Root mean square error is another common statistic that measures the average magnitude of prediction errors. It is the square root of the average of squared differences between predicted and observed target variables values.

$$\text{RMSE} = \sqrt{\frac{1}{n} \sum_{i=1}^{n} \left(y_i - \hat{y}_i \right)^2} \qquad [9]$$

Because the errors are squared before they are averaged, RMSE places high weight to large errors. Thus, it is more sensitive than MAE to large prediction errors. Root mean square error is particularly useful to evaluate model performance when large errors are unwanted.

The performance of each model was evaluated by using leave-one-location-out (LOLO) cross-validation and leave-one-year-out (LOYO) cross-validation (Hastie et al., 2001). Leave-one-out works by iteratively leaving out one site or year from the original dataset as the validation data and using the remaining data to train the model. The model trained on the remaining data is then used to predict EONR for the left-out site or year
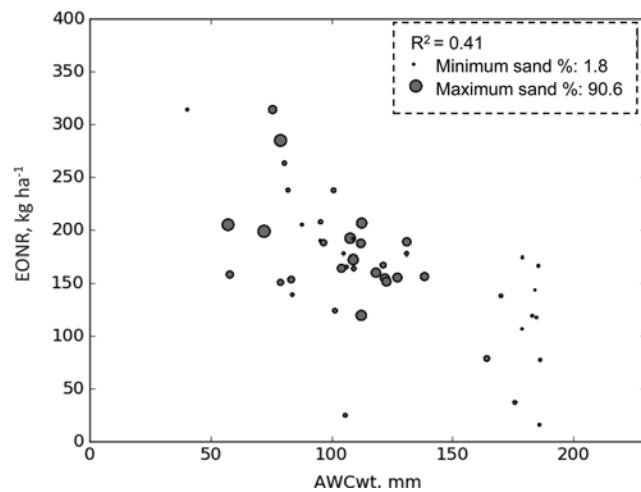

Fig. 1. Split application economic optimum N rate (EONR) for the 47 N response trials declines with increased water table adjusted available water capacity (AWC$_{wt}$). The size of each point represents the percentage of sand at each site.

from the previous step. This process is repeated so that the model validation is iteratively performed for each site or year has been left out of the training process. In the last step, the averaged error is computed and used to evaluate the overall model performance. Leave-one-out cross-validation is especially useful when the size of training data is small.

The model performances are also put into numerical context by comparing them with a "null model" result. The null model, in this case, is the average of the EONR values in the training set. This allows the regression models to be compared with a simple constant model that assumes the target EONR values have no meaningful relationship to the predictor variables.

Site-level EONR values were derived from yield and N data collected from four blocks (replications) within each site. In addition to site-level EONR, block-level EONRs were derived based on yield and N data collected from each block within a site. Variability existed among the block-level EONR within a site due to soil and crop variability. To account for the variation of EONR values within a site, a 95% confidence interval for each site was calculated based on resampled block-level EONR values using a bootstrapping procedure (Beran, 1992). Bootstrapping is a statistical method of resampling (with replacement) that infers population from sample data. It is especially useful when the sample size is insufficient for statistical inference, and the distribution of a statistic is complicated or unknown. Model predicted EONR values were then compared with 95% confidence interval. If the prediction fell into the confidence interval, the prediction was regarded as acceptable; otherwise, it was regarded as failing to predict EONR for that site.

RESULTS AND DISCUSSION
Relationship between AWC$_{wt}$ and EONR

The validity of AWC$_{wt}$ as an N loss indicator was evidenced by its negative relationship with EONR (Fig. 1). Generally, high EONRs are more likely to occur in sandy or sandy loam soils, and low EONRs tend to arise in fine-textured soils with higher clay content because sandy soils are more likely subject to N loss due to leaching. However, there are also some data points with high EONRs and low sand content. These may indicate increased N

Table 5. Waterlogging conditions reported for sites with >200 kg ha⁻¹ split economic optimum N rate from Watermark (placed at 0.30, 0.60, 0.9, and 1.2 m) and Sentek (measured every 0.05 m from the surface) soil moisture sensors. Waterlogging was defined as a soil condition with measured volumetric water content continuously above soil saturation limit for ≥5 days. Soil volumetric water content was obtained by Watermark sensors (2014 and 2016) and Sentek sensors (2015) deployed on the research plots (Kitchen et al., 2017).

Site	Year	Sand content, %	Waterlogging summary
Brownstown	2014	12.7	Waterlogging conditions favorable for denitrification were observed with high precipitation and saturated conditions between the 0 and 0.3 m depth from middle of June through early July measured by watermark sensor (Watermark 200SS; The Irrometer Company, Inc., Riverside, CA).
Urbana	2014	10.1	Waterlogging conditions at 0.3 m depth from tested blocks from early June through middle July. Measured sand content is 4–7% at 0.3 to 0.6 m depth.
Lone Tree	2015	3.9	Waterlogging conditions continuously observed for most of the time during the season from 0.25 to 0.35 m depth using a Senteck sensor (TriSCAN Sensor; Sentek Sensor Technologies, Stepney, SA, Australia). Typical clay-pan soil, confirmed by measured low sand content.
Troth†	2015	39.3	Extended waterlogging above 0.25 m depth during middle June to middle July. High water table caused by the site's proximity to the Missouri River and nearby flooded fields.
Loess	2016	4.4	Waterlogging from 0.3 to 0.6 m depth from May until middle June. Typical clay-pan soil with sand ranging from 3 to 7% across the entire profile for all blocks.
Troth	2016	9.9	Waterlogging observed from 0.3 to 0.6 m depth. Soil samples showed very low sand content (1– 5%) between the 0.2 and 0.5 m depth.

† Waterlogging due to high water table caused by this site's proximity to the Missouri River.

loss due to the greater denitrification that occurs in waterlogged soils. Table 5 lists those high EONR sites (split EONR >200 kg ha⁻¹) where waterlogging happened in near-surface or subsurface soils. Except for the 2015 site at Troth where waterlogging was mainly caused by a high water table due to proximity to the leveed Missouri River, waterlogging was caused by the combined effect of the low sand content of soils and a high water table, which translates to small values of the computed AWC_{wt} feature.

Model Evaluation

In this study, model evaluation was conducted for both at-planting and split N applications with the polynomial order of input features set to 1 and 2. Model performance statistics (R^2, MAE, and RMSE) were reported for all the evaluation scenarios (at planting/split application, polynomial order 1/polynomial order 2). For clarity of interpretation and to see the accuracy of the model at planting and split N application timings, validation results are presented for all of these evaluation scenarios (Table 6).

Among the tested models, LR performed the worst across all evaluation scenarios. When polynomial order p = 1, LR reported R^2 of 0.19 and MAE of 50.6 kg ha⁻¹ for at-planting EONR and R^2 of 0.10 and MAE of 44.8 kg ha⁻¹ for split EONR. The low performance of LR was due to overfitting in the training folds of the cross-validation. This was especially pronounced when the polynomial order was increased to 2 for LR, with no meaningful evaluation statistics generated. Ridge regression and LASSO algorithms both demonstrated better performance than LR. When polynomial order p = 1, RR performed better than LASSO in predicting at-planting EONR, with reported R^2 of 0.41 and MAE of 43.4 kg ha⁻¹. When applied to predict split EONR, performances of both models were much improved. Both RR and LASSO performed similarly with reported R^2 values of 0.41 to 0.43 and MAE of ~34 kg ha⁻¹. As polynomial degree was increased to 2 to account for nonlinear relationships between input and target features, RR performed better than LASSO. For at-planting EONR prediction, RR reported R^2 of 0.41 and MAE of 42.9 kg ha⁻¹, and LASSO reported R^2 of 0.34 and MAE of 46.7 kg ha⁻¹. Ridge regression outperformed LASSO for split EONR prediction as well, with reported R^2 of 0.43 and MAE

Table 6. Comparison of machine learning (ML) algorithms to predict economic optimum N rate (EONR) of corn across 47 sites in the Corn Belt. Model performance using "leave-one-location-out" validation was assessed by R^2, mean absolute error (MAE), and RMSE for scenarios based on at-planting and split N application timings.

Polynomial order	ML algorithm†	At-planting EONR			Split EONR		
		R^2	MAE	RMSE	R^2	MAE	RMSE
			— kg ha⁻¹—			— kg ha⁻¹—	
	Null model		57.4	68.3		43.3	58.2
1	LR	0.19	50.6	65.2	0.10	44.8‡	63.1‡
	RR	0.40	43.4	56.1	0.41	34.1	47.4
	LASSO	0.41	45.3	55.7	0.43	34.0	46.3
	GBRT	0.37	45.5	56.9	0.39	36.8	47.8
2	LR§	–	–	–	–	–	–
	RR	0.41	42.9	55.5	0.43	33.2	46.9
	LASSO	0.34	46.7	58.5	0.41	34.9	47.2
	GBRT	0.39	42.5	56.6	0.40	35.1	47.5

† GBRT, gradient boosted regression trees; LASSO, least absolute shrinkage and selection operator regression; RR, ridge regression.
‡ Model failed to generate a prediction better than a null model (average of target variable in training set).
§ Linear model failed to generate meaningful statistics when the second–degree polynomials were included in the model.

of 33.2 kg ha⁻¹. Across all evaluation scenarios, the GBRT algorithm generally performed better than LR but worse than RR and LASSO algorithms, except for the case of at-planting EONR prediction with p = 2 (Table 6).

It is understandable that EONR models performed better in predicting N application for split versus at-planting applications. As the season progresses from planting to sidedress time (around V9 leaf stage), part of the uncertainty for in-season N management evolves to reality, which makes side-dress EONR more predictable. The fact that the models perform better for split application than they do for planting-time application can also be understood by examining the null model results (Table 6). Because the null model is a pure data–driven approximation of EONR estimation, the lower error of the null model in predicting split EONR logically indicates using an approach such as machine learning would yield similar results (lower MAE/RMSE in predicting split EONR than at planting EONR).
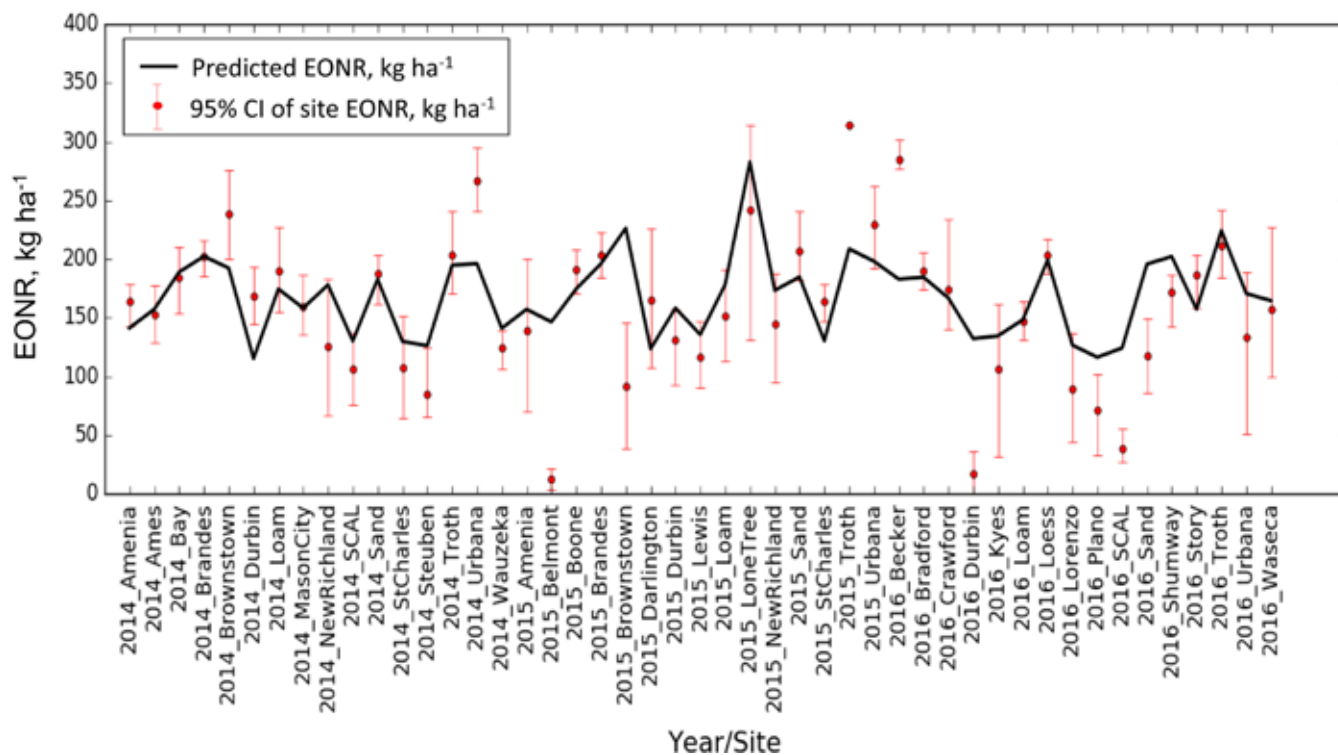
Fig. 2. Comparison of predicted economic optimum N rate (EONR) for sidedress application timing and 95% confidence interval of site EONR across 47 sites in the US Corn Belt. The predicted split EONR for sidedress timing (solid black line) was based on ridge regression (RR) and a polynomial order of 2. The 95% confidence interval for site EONR (red error bar with median value represented by solid red circle) was estimated based on block-level EONR using a bootstrapping procedure. Model performance was evaluated using leave-one-location-out validation. Mean absolute error was 33.2 kg N ha^{-1} and R^2 = 0.43.

Incorporation of polynomial terms of input features helped improve the performance of the tested RR and GBRT algorithms (Table 6). This suggests the existence of nonlinear relationships between input features and the target variable (EONR) was captured by RR and GBRT models. The LASSO algorithm, however, did not benefit from the incorporation of polynomial terms of input features.

Considering the existence of soil and crop condition variability within a site, site-specific EONR predictions need to be evaluated in the context of variability among the block-level EONR within a site. Figure 2 shows the predicted split EONR based on RR and polynomial order of 2 and the 95% confidence intervals of site EONRs. Among the 47 testing sites, the predicted EONR for 33 sites fell into the 95% confidence interval of the site EONR, suggesting the model made acceptable predictions for 70% of testing sites. Among the 14 sites that had predicted EONR values that fell outside of the confidence interval, there were three with no or little N observed in the EONR response (Belmont 2015, Durbin 2016, SCAL 2016). Clearly, the model failed to make good predictions of EONR for these sites. We checked the data collected from these locations, but no unique conditions could explain the extremely low EONR values. With these three sites removed from the dataset, LOLO validation improved with a predicted split EONR with an R^2 of 0.44 and MAE of 28.3 kg ha^{-1}. This suggests that some unique soil/crop conditions might have been missed from these sites that would help to explain the crop's lack of response to added N.

On the other hand, field notes and data of in-season soil moisture measurements helped explain why the model failed to predict high EONRs observed at some sites. One example was the Troth

site, which experienced waterlogging during early and middle summer of 2015 due to its proximity to the Missouri River. At this site, high water levels may have contributed to denitrification and slowed plant growth. This condition undoubtedly helps explain why the model underpredicted EONR. A similar situation happened at Brownstown 2014, Urbana 2014, and a few other sites (Table 5) where clayey soils and heavy rain raised the water table. Extended waterlogging on these sites potentially caused low soil N concentration from denitrification and/or anaerobic conditions that inhibit crop uptake of N. An important input feature to predict EONR, AWC$_{wt}$, was computed based on water table depth reported from the SSURGO database, which may not capture seasonal variability of the water table depth at a specific location. In addition to the issue with water table depth estimate, other documented or undocumented biotic and abiotic stresses, such as disease or wind/hail damage, occurred at a few other sites and may also have contributed to the model prediction error. Given the plot size of the N trials had been large enough, those biotic and abiotic stresses could have been captured by near real-time remotely sensed imagery data. To enhance the model predictability, we recommend incorporating monitored in-season soil water (especially water table depth) and crop conditions in future research in modeling EONR.

Table 7 presents cross-validation results using a LOYO approach. This approach was used to evaluate the stability of tested models in capturing the yearly variation of environments. The model performance varied among the 3 yr: GBRT outperformed RR and LASSO in predicting both at planting and split EONR for 2014 and 2015, LASSO made a better prediction for at planting EONR for 2016, and RR outperformed other two

models to predict split EONR for 2015. All three algorithms consistently underperformed in predicting at planting and split EONRs for 2015, with reported MAE ranging from 41 to 47 kg ha^{-1} for split EONR prediction and from 62 to 66 kg ha^{-1} for at-planting EONR prediction. This underperformance is likely due to unique field situations that happened on a few sites in 2015 not well represented by the models, as discussed above. The outperformance of the three models for predicting EONR for 2014 (MAE of 29–35 kg ha^{-1} for at planting prediction, MAE of 22–27 kg ha^{-1} for split prediction) is probably due to the absence of those extremely low N response sites.

Even if RR did not perform the best in LOYO validation, considering the training data for LOYO validation was only two-thirds of that used for LOLO validation, RR is still regarded as a preferred model for EONR prediction with this dataset.

Modeling Consideration Discussion

Economic optimum N rate is a function of G × E × M, which can be presented as:

$$EONR = f(G, E, M) \qquad [10]$$

All terms in Eq. [10] are known to have strong interactions leading to complicated nonlinear relationships.

There are multiple ways to construct a solution for a system such as Eq. [10]: these include mechanistic and empirical approaches. A mechanistic approach assumes that a system can be understood by defining the form and functions of individual parts of the system and the mechanism of how they are coupled. Therefore, a mechanistic model solves the target variable or output by explicitly determining all initial and intermediate parameters. The empirical approach, on the other hand, uses a statistical approach to approximate the target variables based on empirical observations rather than on mathematically describable relationships. Mechanistic modeling is preferred if all important processes and variables required to describe the system can be explicitly determined or mathematically defined. If a system is difficult to mathematically describe due to the uncertainty involved in determining input variables and/or relationships, an empirical model may be preferred.

In a complex agronomic system, uncertainty exists in some input variables and relationships among the variables. However, certain components of the system can be explicitly described using domain knowledge. In this situation, mechanistic modeling complements empirical modeling to solve a complex problem. For modeling EONR, in-season soil N dynamics are determined by multiple interacting processes divided into soil N losses (leaching, denitrification, crop uptake, etc.) and N gains (soil mineralization, N fertilizer application, etc.), which cannot be easily measured or simulated using a simplistic and reliable model. On the other hand, mechanistic features based on agronomic domain knowledge does contain information that correlates to in-season N loss and gain. In this study, AWC$_{wt}$ and RAWC$_{wt}$ are essentially correlative mechanistic features. They represent interactions between the amount of water that can be held by soil and other key limits to that capacity. This analysis demonstrated that it was advantageous to include soil-process components in empirical modeling of EONR because these derived features combine soil properties and weather information to better explain N loss and

Table 7. Comparison of machine learning (ML) algorithms to predict economic optimum N rate (EONR) of corn across 47 sites in the Corn Belt. Model performance using leave-one-year-out validation (LOYO) was assessed by R^2, mean absolute error (MAE), and RMSE for scenarios based on N applied at-planting and side-dress application timing. Second-order polynomial (p = 2) terms of input features were used for LOYO cross-validation due to improved model performance. Evaluation of linear regression is not presented in this table because it failed to generate meaningful statistics when p = 2.

Year	ML algorithm†	At-planting EONR			Split EONR		
		R^2	MAE	RMSE	R^2	MAE	RMSE
			— kg ha^{-1}—			— kg ha^{-1}—	
2014	RR	0.37	34.9	46.2	0.35	27.2	35.5
	LASSO	0.38	35.0	45.7	0.48	25.8	31.5
	GBRT	0.58	29.4	37.7	0.60	22.0	27.8
2015	RR	0.21	62.5	72.3	0.39	41.4	56.8
	LASSO	0.15	66.5	74.9	0.31	46.7	60.4
	GBRT	0.23	60.5	71.3	0.35	41.9	58.4
	RR	0.43	46.1	55.1	0.32	40.8	52.4
2016	LASSO	0.48	44.8	52.1	0.43	37.1	47.7
	GBRT	0.31	47.9	60.4	0.43	37.0	47.8

† GBRT, gradient boosted regression trees; LASSO, least absolute shrinkage and selection operator regression; RR, ridge regression.

gain, which is well illustrated in Fig. 3, where EONR is shown as a function of the mechanistically derived AWC$_{wt}$ and RAWC$_{wt}$.

In-Season Model Testing Using Historic Weather

Machine learning–based EONR models presented in this study were trained and validated using the weather data of the entire season (from planting to maturity). However, for real-world application of this model, weather data for the rest of season are unavailable at time of N application. Creation of the weather feature matrices for in-season model testing was previously detailed. In total, 10 input weather feature matrices were created based on historical weather data from the previous 10 yr across all study sites. The engineered historical weather feature matrices were further integrated with soil and management features to form complete input feature matrices. To objectively evaluate the model performance for a real-world application, LOLO calibration was adopted to iteratively predict EONR for each of the site–historical year combinations using the model optimized through LOLO cross validation, which was based on data from remaining sites.

Box-whisker plots show predicted EONR values by site based on the RR algorithm and a polynomial level of 2 using real weather data up to the time of sidedress and historical weather data after sidedress (Fig. 4). The mean value of the 10 predicted EONR values for each site was compared with the observed EONR for calculation of comparison statistics. Performance of the model based on the actual weather for the entire season or using historical data post sidedress, resulted in similar R^2 (0.43 vs. 0.46) and MAE (33.2 kg ha^{-1} vs. 33.6 kg ha^{-1}). This suggests stable N recommendation when the model is applied at sidedress time (V9 ± 1 leaf stage).

CONCLUSION

This study applied ML methodologies to predict planting time and split EONR. To support model development, an input
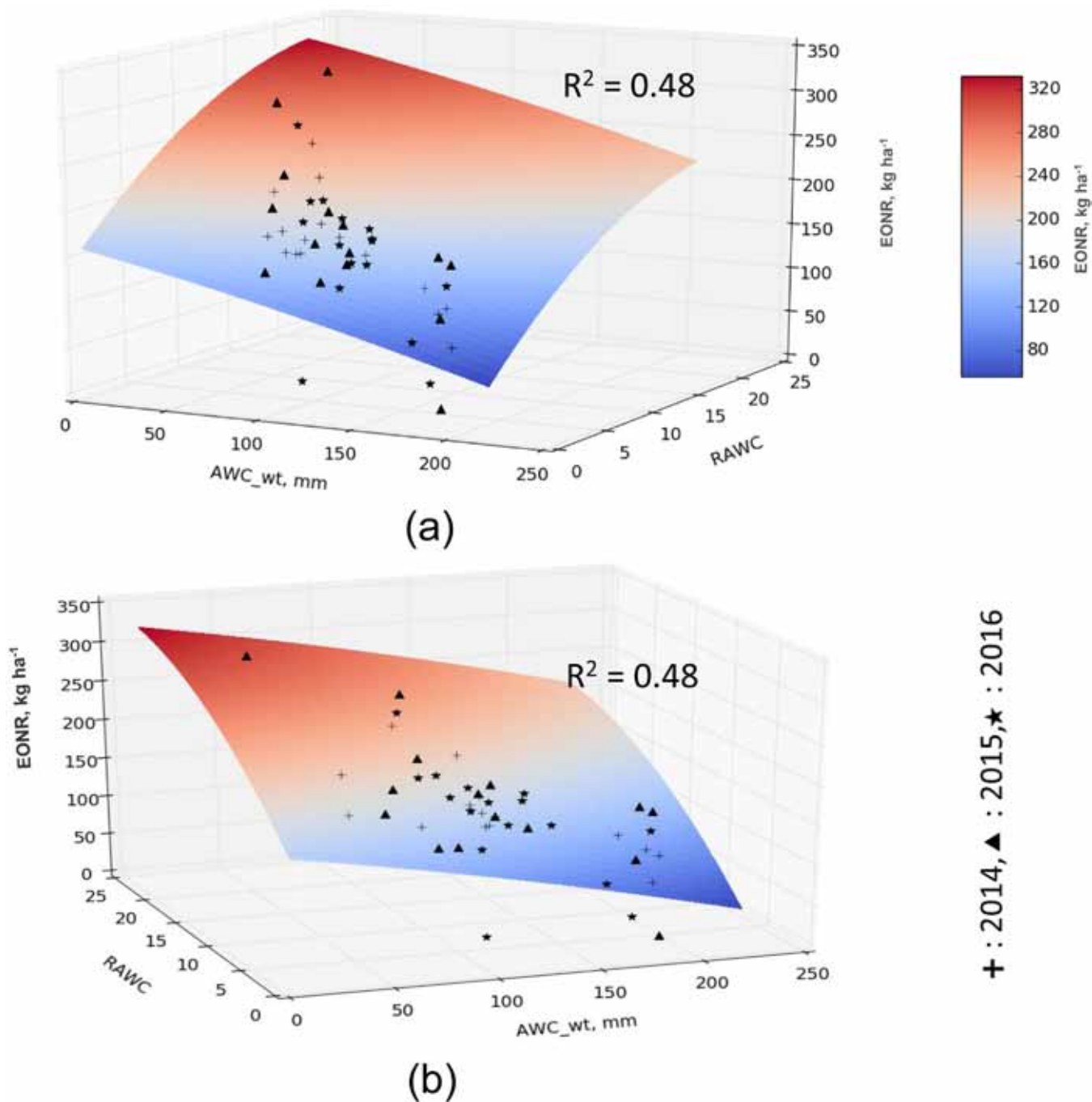
Fig. 3. Illustration of economic optimum N rate (EONR) modeling concept. The *x* and *y* axis in this chart are water table adjusted available water capacity (AWC$_{wt}$) and ratio of in-season rainfall to AWC$_{wt}$ (RAWC$_{wt}$), respectively. The z axis is EONR in kg N ha^{-1}. The curved surface represents quadratic model of EONR fitted by the observational data. Data points represent observed split EONRs from the 47 sites for 2014, 2015, and 2016. (a) and (b) display the same 3-D chart from two different perspectives.

feature matrix was derived based on raw field measurements and domain knowledge. Four ML algorithms, LR, RR, LASSO, and GBRT were evaluated against EONR derived from yield and N measurements from 2014 to 2016 through LOLO and LOYO cross-validation. Ridge regression marginally performed better in predicting planting time and split EONR than LASSO and GBRT algorithms in LOLO cross-validation. In LOYO validation, model performances varied depending on evaluation scenarios. Among all tested algorithms, LR performed the worst due to lack of regularization to correct model overfitting.

We evaluated EONR prediction using the RR model using the 95% confidence interval of site EONR, computed based

on block-level EONR values using a bootstrapping resampling procedure. Among the 47 tested sites, for 33 sites the predicted split EONR using RR fell within the 95% confidence interval, suggesting the chances of using the RR model to make an acceptable prediction of split EONR is around 70%. The RR model failed in predicting extremely low EONR values for three sites where no special situations were identified in the environmental and crop data. Prediction errors for other sites were mainly due to inaccurate estimates of in-season water table depth by using SSROGO database or in-season biotic and abiotic anomalies that were not captured with the data collection. Incorporation of in-season monitored information of soil water
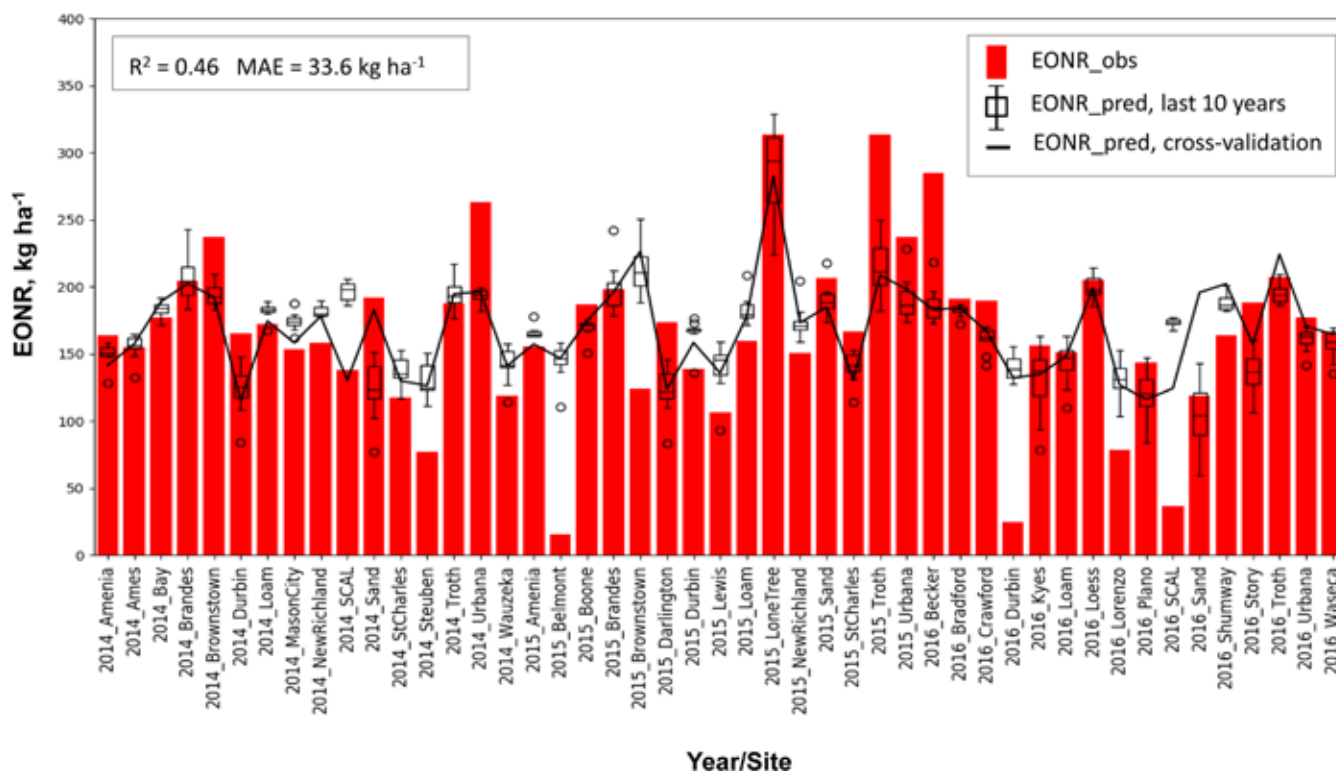
Fig. 4. Comparison of measured economic optimum N rates (EONR) for split application timing of corn for 47 sites in the US Corn Belt (red bars) and predicted EONR based on ridge regression (RR) and a polynomial order of 2 using historical weather data after sidedress date (represented by box and whiskers). The box midline represents the median, the upper and lower edges of the box represent the 25th and 75th percentiles, and the whiskers represent the range where outlier is absent and the 1.5′ interquartile range when outlier is present, and the circles outside the whiskers represent outliers. Predicted EONR values using actual weather at cross-validation presented for comparison (black line).

and crop condition could potentially improve EONR model predictability.

To assess model performance at the time of sidedress under real-world situations, when future weather data are unavailable, it was an effective strategy to combine historical weather data with the current season's weather. This also enabled evaluating the uncertainty of the prediction based on the range of weather outcomes represented by the historical data. The RR algorithm selected in this study displays robustness in predicting split application EONR, with R^2 values of 0.46 and MAE of 33.6 kg ha^{-1}.

Incorporating mechanistically derived soil hydrological features significantly enhanced the ability of the ML procedures to model EONR. Two input features, AWC_{wt} and $RAWC_{wt}$, could capture the effect of soil hydrologic conditions on N dynamics. Improvement in estimating in-season soil hydrological status seems essential for success in modeling N demand.

The models developed in this study were based on data collected from a limited number of research sites when it comes to ML standards, which may insufficiently represent the corn-growing environments in the Midwest and the complexity of G × E × M outcomes. Some features that may be relevant to EONR, such as crop rotation, genetic variability in N response, and tillage, were not used by the model due to a relatively small number of trials. Improvement of ML-derived models for predicting EONR will require more data from many more diverse environments and management scenarios than reported in this paper. Because the data for this analysis were collected from small research plots (~0.4 ha per site) to minimize variability in the EONR measurement, validation at production-scale fields is needed.

REFERENCES

Barker, D.W., and J.E. Sawyer. 2010. Using active canopy sensors to quantify corn nitrogen stress and nitrogen application rate. Agron. J. 102:964–971. doi:10.2134/agronj2010.0004

Basso, B., L. Sartori, D. Cammarano, C. Fiorentino, P.R. Grace, S. Fountas, and C.A. Sorensen. 2012. Environmental and economic evaluation of N fertilizer rates in a maize 15 crop in Italy: A spatial and temporal analysis using crop models. Biosystems Eng. 113:103–111. doi:10.1016/j.biosystemseng.2012.06.012

Beran, R.J. 1992. Introduction to Efron (1979) bootstrap methods: Another look at the jackknife. Springer, New York.

Bristow, K.L., and G.S. Campbell. 1984. On the relationship between incoming solar radiation and daily maximum and minimum temperature. Agric. For. Meteorol. 31:159–166. doi:10.1016/0168-1923(84)90017-0

Chen, T., and C. Guestrin. 2016. XGBoost: A scalable tree boosting system. Paper presented at KDD'16 Proceedings of the 22nd ACM SIGKDD International Conference on Knowledge Discovery and Data Mining, San Francisco, CA. 13-17 Aug. doi:10.1145/2939672.2939785

Commission for Environmental Cooperation. 1997. Ecological regions of North America: Toward a common perspective. Commission for Environmental Cooperation, Montreal, Quebec, Canada.

Dahnke, W.C., and E.H. Vasey. 1973. Testing soils for nitrogen. In: L.M. Walsh and J.D. Beaton, editors, Soil testing and plant analysis. SSSA, Madison, WI. p. 97–114.

Dellinger, A.E., J.P. Schmidt, and D.B. Beegle. 2008. Developing nitrogen fertilizer recommendations for corn using an active sensor. Agron. J. 100:1546–1552. doi:10.2134/agronj2007.0386

Dumont, B., B. Basso, B. Bodson, J.P. Destain, and M.F. Destain. 2016. Assessing and modeling economic and environmental impact of wheat nitrogen management in Belgium. Environ. Model. Softw. 79:184–196. doi:10.1016/j.envsoft.2016.02.015

Gonzalez-Sanchez, A., J. Frausto-Solis, and W. Ojeda-Bustamante. 2014. Predictive ability of machine learning methods for massive crop yield prediction. Span. J. Agric. Res. 12:313–328. doi:10.5424/sjar/2014122-4439

Guyon, I., J. Weston, S. Barnhill, and V. Vapnik. 2002. Gene selection for cancer classification using support vector machines. Mach. Learn. 46:389–422. doi:10.1023/A:1012487302797

Hastie, T., R. Tibshirani, and J.H. Friedman. 2001. The elements of statistical learning: Data mining, inference, and prediction. Springer. New York doi:10.1007/978-0-387-21606-5

Holland, K.H., and J.S. Schepers. 2013. Use of a virtual-reference concept to interpret active crop canopy sensor data. Precis. Agric. 14:71–85. doi:10.1007/s11119-012-9301-6

Jeong, J.H., J.P. Resop, N.D. Mueller, D.H. Fleisher, K. Yun, E.E. Butler et al. 2016. Random forests for global and regional crop yield predictions. PLoS One, 11(6):e0156571. doi:10.1371/journal.pone.0156571

Karimi, Y., S.O. Prasher, A. Madani, and S. Kim. 2008. Application of support vector machine technology for the estimation of crop biophysical parameters using aerial hyperspectral observations. Canadian Biosyst. Eng. 50:13–20.

Kitchen, N.R., J.F. Shanahan, C.J. Ransom, C.J. Bandura, G.M. Bean, J.J. Camberato, et al. 2017. A public–industry partnership for enhancing corn nitrogen research and datasets: Project description, methodology, and outcomes. Agron. J. 109:2371–2388. doi:10.2134/agronj2017.04.0207

Kitchen, N.R., K.A. Sudduth, S.T. Drummond, P.C. Scharf, H.L. Palm, D.F. Roberts, and E.D. Vories. 2010. Ground-based canopy reflectance sensing for variable-rate nitrogen corn fertilization. Agron. J. 102:71–84. doi:10.2134/agronj2009.0114

Lukina, E.V., K.W. Freeman, K.J. Wynn, W.E. Thomason, R.W. Mullen, M.L. Stone, et al. 2001. Nitrogen fertilization optimization algorithm based on in-season estimates of yield and plant nitrogen uptake. J. Plant Nutr. 24:885–898. doi:10.1081/PLN-100103780

Ma, B.L., K.D. Subedi, and C. Costa. 2005. Comparison of crop-based indicators with soil nitrate test for corn nitrogen requirement. Agron. J. 97:462–471. doi:10.2134/agronj2005.0462

Magdoff, F., D. Ross, and J. Amadon. 1984. A soil test for nitrogen availability to corn. Soil Sci. Soc. Am. J. 48:1301–1304. doi:10.2136/sssaj1984.03615995004800060020x

McQueen, R., S. Garner, C. Nevill-Manning, and I. Witten. 1995. Applying machine learning to agricultural data. Comput. Electron. Agric. 12:275–293. doi:10.1016/0168-1699(95)98601-9

Melkonian, J.J., H.M. van Es, A.T. DeGaetano, and L. Joseph. 2008. ADAPT-N: Adaptive nitrogen management for maize using high resolution climate data and model simulations. In: R. Khosla, editor, Proceedings 9th International Conference on Precision Agriculture, Denver, CO. 18–21 July 2010. International Soc. Precision Agric., Monticello, IL.

Morellos, A., X. Pantazi, D. Moshou, T. Alexandridis, R. Whetton, G. Tziotzios, J. Wiebensohn, R. Bill, and A. Mouazen. 2016. Machine learning based prediction of soil total nitrogen, organic carbon and moisture content by using VIS-NIR spectroscopy. Biosystems Eng. 152:104–116. doi:10.1016/j.biosystemseng.2016.04.018

Morris, T., T.S. Murrell, D.B. Beegle, J. Camberato, R. Ferguson, J. Grove, et al. 2018. Strengths and limitations of nitrogen recommendations, tests and models for corn. Agron. J. 110:1–37. doi:10.2134/agronj2017.02.0112

Puntel, L., J. Sawyer, D. Barker, R. Dietzel, H. Poffenbarger, M. Castellano, K. Moore, P. Thorburn, and S. Archontoulis. 2016. Modeling long-term corn yield response to nitrogen rate and crop Rotation. Front. Plant Sci. 7:1630. doi:10.3389/fpls.2016.01630

Raun, W.R., J.B. Solie, G.V. Johnson, M.L. Stone, E.V. Lukina, W.E. Thomason, and J.S. Schepers. 2001. In-season prediction of potential grain yield in winter wheat using canopy reflectance. Agron. J. 93:131–138. doi:10.2134/agronj2001.931131x

Raun, W.R., J.B. Solie, G.V. Johnson, M.L. Stone, R.W. Mullen, K.W. Freeman, et al. 2002. Improving nitrogen use efficiency in cereal grain production with optical sensing and variable rate application. Agron. J. 94:815–820. doi:10.2134/agronj2002.8150

Rhezali, A., L. Purcell, T. Roberts, and C. Greub. 2018. Predicting nitrogen requirements for maize with the dark green color index under experimental conditions. Agron. J. 110:1173–1179. doi:10.2134/agronj2017.09.0543

Rokach, L., and O. Maimon. 2008. Data mining with decision trees: Theory and applications. World Scientific Pub. Co. Singapore.

Rumpf, T., A. Mahlein, U. Steiner, E. Oerke, H. Dehne, and L. Plümer. 2010. Early detection and classification of plant diseases with Support Vector Machines based on hyperspectral reflectance. Comput. Electron. Agric. 74:91–99. doi:10.1016/j.compag.2010.06.009

Samuel, A.L. 1959. Some studies in machine learning using the game of checkers. IBM J. R. D. 3:210–229. doi:10.1147/rd.33.0210

Sawyer, J., E. Nafziger, G. Randall, L. Bundy, G. Rehm, and B. Joern. 2006. Concept and rationale for regional nitrogen rate guidelines for corn. Iowa State Univ. Ext., Ames.

Saxton, K.E., and W.J. Rawls. 2006. Soil water characteristic estimates by texture and organic matter for hydrologic solutions. Soil Sci. Soc. Am. J. 70:1569–1578. doi:10.2136/sssaj2005.0117

Scharf, P.C. 2001. Soil and plant tests to predict optimum nitrogen rates for corn. J. Plant Nutr. 24:805–826. doi:10.1081/PLN-100103775

Scharf, P.C., and J.A. Lory. 2009. Calibrating reflectance measurements to predict optimal sidedress nitrogen rate for corn. Agron. J. 101:615–625. doi:10.2134/agronj2008.0111

Schmidt, J.P., A.E. Dellinger, and D.B. Beegle. 2009. Nitrogen recommendations for corn: An on-the-go sensor compared with current recommendations. Agron. J. 101:916–924. doi:10.2134/agronj2008.0231x

Setiyono, T.D., H. Yang, D.T. Walters, A. Dobermann, R.B. Ferguson, D.F. Roberts, et al. 2011. Maize-N: A decision tool for nitrogen management in maize. Agron. J. 103:1276–1283. doi:10.2134/agronj2011.0053

Shekoofa, A., Y. Emam, N. Shekoufa, M. Ebrahimi, and E. Ebrahimie. 2014. Determining the most important physiological and agronomic traits contributing to maize grain yield through machine learning algorithms: A new avenue in intelligent agriculture. PLoS One 9(5):e97288. doi:10.1371/journal.pone.0097288

Schepers, J.S., F.D. Frank, and C. Bourg. 1986. Effect of yield goal and residual soil nitrogen considerations on nitrogen fertilizer recommendations for irrigated maize in Nebraska. J. Fert. 3:133–139.

Snoek, J., H. Larochelle, and R.P. Adams. 2012. Practical Bayesian optimization of machine learning algorithms. NIPS'12 Proceedings of the 25th International Conference on Neural Information Processing Systems. V2(2951-2959). Lake Tahoe, Nevada. 3–6 Dec. 2012.

Tremblay, N., M.Y. Bouroubi, C. Bélec, R. Mullen, N. Kitchen, W. Thomason, et al. 2012. Corn response to nitrogen is influenced by soil texture and weather. Agron. J. 104:1658–1671. doi:10.2134/agronj2012.0184

Tubaña, B.S., D.B. Arnall, O. Walsh, B. Chung, J.B. Solie, K. Girma, and W.R. Raun. 2008. Adjusting midseason nitrogen rate using a sensor-based optimization algorithm to increase use efficiency in corn. J. Plant Nutr. 31:1393–1419. doi:10.1080/01904160802208261

Wei, J., C. Messina, S. Langton, Z. Qin, A. Perdomo, and C. Loeffler. 2009. Predictability of CERES-Maize for flowering date. ASA, CSSA, and SSSA Annual Meetings, Pittsburgh, PA. 1–5 Nov. 2009. Paper 702-9.

Xie, M., N. Tremblay, G. Tremblay, G. Bourgeois, M. Bouroubi, and Z. Wei. 2013. Weather effects on corn response to in-season nitrogen rates. Can. J. Plant Sci. 93:407–417. doi:10.4141/cjps2012-145